FLOW INDUCED FORCE OF LABYRINTH SEAL

Takuzo Iwatsubo, Naoto Motooka,
and Roji Kawai
Faculty of Engineering, Kobe University
Rokko, Nada, Kobe, 657 Japan

SUMMARY

This paper deals with theoretical analysis of flow induced instability force due to labyrinth seal. That is, a approximate solution is given for the partial differential equation representing the flow in labyrinth seal and it is compared with the finite difference method which was proposed in the previous report in order to verify the accuracy of both methods. Then the effects of difference of inlet and outlet pressures of the seal, deflection of pressure and mass flow from the steady state, rotor diameter, seal clearance, seal interval and seal number on the flow induced force of the seal are investigated and it is known that some of these factors are very influential on the flow induced force.

INTRODUCTION

In the previous report (1), the fundamental equation of flow in the labyrinth seal was derived by considering the effect of the variation of gland cross section. The equation is numerically solved by using the finite difference method. Then the spring and damping coefficients of the labyrinth seal are calculated, and by using the result, the stability of a rotor system having labyrinth seal is discussed on this coefficient by using the energy concept. Furthermore, experiments are executed to observe the flow pattern in the gland and to study the characteristics of the flow induced forces in the labyrinth seal.

However, further theoretical investigations are required for the accuracy of numerical calculation and more detail description of labyrinth seal behaviour. Then in this paper the equation is solved by another method and the calculated results are compared with the solution of finite difference method. After that influences of deflection of steady state, pressure difference between inlet and outlet, labyrinth seal radius, seal clearance, seal pitch, number of seal chamber, seal strip height and divergence and convergence seal on the flow induced force, phase angle and leakage flow rate are investigated.

SYMBOLS

t   time

w   = $R_s \varphi$

R_s radius of labyrinth seal

p   pressure in seal chamber

c	peripheral velocity in seal chamber
ρ	density of gas
q	mass flow rate in axial direction
φ	angle from x axis
f	cross section of seal chamber
ℓ	length of strip pitch
h	strip height
δ	radial clearance of seal
τ'	friction shear stress of stator surface
τ''	friction shear stress of rotor surface
U'	length of acting surface of shear stress (stator)
U"	length of acting surface of shear stress (rotor)
R	gas constant
T	absolute temperature of gas in seal
γ	specific weight of gas
ψ	flow coefficient
n	ratio of specific heat
ω	rotating speed of rotor
ω_n	critical speed of rotor system
$u = \omega R_s$	peripherical velocity of rotor
K	coefficient of viscosity
ν	coefficient of kinematic viscosity
R_e	Reynold's number
λ'	friction coefficient (stator)
λ''	friction coefficient (rotor)
subscript *	steady state

EQUATION OF MOTION

Derivation of Equation of Motion

Derivation of the equation which describes the labyrinth seal flow is followed the previous report (1), where the following assumptions are taken and schematic flow is shown in Fig.1;

(1) Fluid in labyrinth seal is assumed to be gas and its behavior is assumed to be ideal.

(2) Temperature of the fluid in the labyrinth seal is assumed to be constant.

(3) Cross section area of the seal gland is assumed to be constant in spite of the deflection of rotor and time derivative of cross section area is only considered.

(4) Change of flow state in the gland is assumed to be isentropic change. Thus the fundamental equations with respect to continuity and momentum for the ith seal element are as follows;

$$\frac{\partial(\rho_i f_i)}{\partial t} + f_i \frac{\partial(\rho_i c_i)}{\partial w} + (g_{i+1} - g_i) = 0 \tag{1}$$

$$f_i \frac{\partial(\rho_i c_i^2)}{\partial w} + \frac{\partial(\rho_i f_i c_i)}{\partial t} + (g_{i+1} c_i - g_i c_{i-1}) + \tau_i' U_i' - \tau_i'' U_i'' = -\frac{\partial p_i}{\partial w} f_i \tag{2}$$

As temperature of each gland is constant, the equation of state in the ith gland is given as;

$$p_i = \gamma_i R T \tag{3}$$

where

$$\gamma_i = \rho_i g$$

Next, denoting the gas flow velocity through labyrinth nozzle (seal clearance) S, the relation between axial flow rate and pressure in the gland is given by the thermodynamical energy equilibrium condition as,

$$S = \sqrt{2g \frac{n}{n-1} p_I v_I \left[1 - \left(\frac{p_0}{p_I}\right)^{\frac{n-1}{n}}\right]} \tag{4}$$

where n is isentropic exponent, v specific volume and subscripts I and 0 mean inlet and outlet of nozzle, respectively. Assuming that the flow is adiabatic change, i.e. $v_0 = (p_I / p_0)^{\frac{1}{n}} \times v_I$, the flow rate through the nozzle G [kgf/sec] is given as;

$$G = \alpha \frac{F \cdot S}{v_0} = \alpha \frac{F \cdot S}{v_I} \left(\frac{p_0}{p_I}\right)^{\frac{1}{n}} = \alpha F \sqrt{2g \frac{n}{n-1} \frac{p_I}{v_I} \left[\left(\frac{p_0}{p_I}\right)^{\frac{2}{n}} - \left(\frac{p_0}{p_I}\right)^{\frac{n+1}{n}}\right]} \tag{5}$$

where F is nozzle cross area (area of seal clearance) and subscripts (i,0) correspond to the gland number of the labyrinth seal. Applying the above relation to flow in the labyrinth seal, we assume that the labyrinth seal is a series of the nozzle, pressure difference between each gland is small and enthalpy of each gland is nearly equal. Then leakage flow rate through labyrinth seal G (kgf/sec) is given by using the relation
$p_1 v_1 = p_2 v_2 = \cdots = p_i v_i$ as;

$$G_L = \alpha F \sqrt{\frac{g}{RT}} \sqrt{P_I^2 - P_0^2}$$ (6)

Applying Eq.(6) to the flow through the ith seal element, mass flow rate for unit area is given as;

$$\frac{q_i}{\delta_i} = \frac{G_L}{F \cdot g} = \frac{\alpha}{\sqrt{g RT}} \sqrt{P_{i-1}^2 - P_i^2}$$ (7)

Rewriting Eq.(7), the following equation is obtained;

where
$$P_{i-1}^2 - P_i^2 = \frac{q_i^2}{\mu^2 \delta_i^2}$$ (8)

$$\frac{1}{\mu^2} = \frac{g RT}{\alpha^2}$$ (9)

Linearization of Fundamental Equation

For the linearization of the equation, the perturbations of pressure, peripheral velocity and flow rate from those of the steady state and also mean value and perturbation of seal clearance are introduced as

$$P_i = P_{*i}(1 + \xi_i) \qquad C_i = C_{*i}(1 + \eta_i)$$
$$q_i = q_{*i}(1 + \zeta_i) \qquad \delta_i = \delta_{*i}(1 + \psi_i)$$ (10)

where p_{*i}, c_{*i} and q_{*i} are pressure, peripheral velocity and axial flow rate of steady state in the ith gland and ξ_i, η_i and ζ_i are nondimensional perturbation terms of pressure, peripheral velocity and axial flow rate. Also δ_{*i} and ψ_* are mean value and perturbation of seal clearance.

Assuming that the rotor is whirling along elliptical orbit, ψ_i is represented as

$$\psi_i = -\frac{a_i}{\delta_{*i}} \cos \omega t \cos \varphi - \frac{b_i}{\delta_{*i}} \sin \omega t \sin \varphi$$ (11)

Then the cross section area in the ith gland is represented as

$$f_i = \left\{ h_i + \delta_{*i}(1 + \psi_i) + h_{i+1} + \delta_{*i+1}(1 + \psi_{i+1}) \right\} \frac{\ell}{2} \tag{12}$$

As the change of state in the gland is isentropic, the following relations are obtained;

$$\frac{P_{*i}}{\rho_{*i}^n} = \frac{P_i}{\rho_i^n} = A \tag{13}$$

therefore

$$\frac{\partial P_i}{\partial t} = n \frac{P_i}{\rho_i} \frac{\partial \rho_i}{\partial t} \tag{14}$$

Substituting Eqs.(10) - (14) into Eqs.(1) and (2), and denoting the time derivative $\frac{\partial}{\partial t}$ and spatial derivative $\frac{\partial}{\partial \varphi}$ ($\dot{\,}$) and ($\cdot$)', respectively, the following equations are obtained for the ith seal element;

$$\frac{f_{*i}}{n} \dot{\xi}_i + \frac{C_* f_{*i}}{nRs} \xi_i' + \frac{C_* f_{*i}}{Rs} \eta_i' - \frac{gRTP_{*i}^2 \delta_{*i+1}^2 \mu^2}{g_* P_{*i}} \xi_{i+1} + \frac{gRT\mu^2 P_{*i}}{g_*} (\delta_{*i+1}^2 + \delta_{*i}^2)\xi_i$$

$$- \frac{gRTP_{*i-1}^2 \delta_{*i}^2 \mu^2}{g_* P_{*i}} \xi_{i-1} + \frac{gRT\mu^2 \delta_{*i+1}}{2 P_{*i} g_*} (P_{*i}^2 - P_{*i+1}^2) - \frac{gRT\mu^2 \delta_{*i} P_{*i-1}^2}{2 P_{*i} g_*} (P_{*i-1}^2 - P_{*i}^2)$$

$$= \frac{gRT\mu^2}{g_* P_{*i}} \delta_{*i+1} (P_{*i}^2 - P_{*i+1}^2)\{a_{i+1}\cos\omega t \cos\varphi + b_{i+1}\sin\omega t \sin\varphi\}$$

$$- \frac{gRT\mu^2}{g_* P_{*i}} \delta_{*i} (P_{*i-1}^2 - P_{*i}^2)\{a_i\cos\omega t \cos\varphi + b_i \sin\omega t \sin\varphi\}$$

$$+ \frac{\ell}{2}\{-a_i\omega\sin\omega t \cos\varphi + b_i\omega\cos\omega t \sin\varphi - a_{i+1}\omega\sin\omega t \sin\varphi + b_{i+1}\omega\cos\omega t \sin\varphi\} \tag{15}$$

$$\frac{f_{*i}}{n} \dot{\xi}_i + f_{*i}\dot{\eta}_i + \frac{f_{*i}}{Rs} \left(\frac{gRT}{C_{*i}} + \frac{C_{*i}}{n}\right)\xi_i' + \frac{C_{*i} f_{*i}}{Rs} \eta_i' - \frac{gRT\mu^2 \delta_{*i+1}^2 P_{*i+1}^2}{g_* P_{*i}} \xi_{i+1}$$

$$+ \left\{ \frac{gRT\mu^2 \delta_{*i+1}^2 P_{*i}}{g_*} + \frac{gRT\mu^2 \delta_{*i}^2 P_{*i}}{g_*} + \frac{\lambda_i' C_{*i} U_i'}{2} - \frac{\lambda_i' U_i'}{2C_{*i}} (u - C_{*i})^2 \right\} \xi_i$$

$$+ \left\{ \frac{gRT g_*}{P_{*i}} + \lambda_i' C_{*i} U_i' + \lambda_i' U_i''(u - C_{*i}) \right\}\eta_i - \frac{gRT\mu^2 \delta_{*i} P_{*i-1}}{g_* P_{*i}} \xi_{i-1} - \frac{gRT g_*}{P_{*i}} \eta_{i-1}$$

$$+ \frac{\lambda_i' C_{*i} U_i'}{2} - \frac{\lambda_i'' U_i''}{2C_{*i}} (u - C_{*i})^2 + \frac{gRT\mu^2}{2g_*} \left(\delta_{*i+1}^2 P_{*i} - \delta_{*i+1}^2 \frac{P_{*i+1}^2}{P_{*i}} - \delta_{*i}^2 \frac{P_{*i-1}^2}{P_{*i}} + \delta_{*i}^2 P_{*i}\right)$$

$$= \frac{gRT\mu^2}{g_*} \left[\left(\delta_{*i} P_{*i} - \delta_{*i+1} \frac{P_{*i+1}^2}{P_{*i}}\right)(a_{i+1}\cos\omega t \cos\varphi + b_{i+1}\sin\omega t \sin\varphi) \right.$$

$$- \left(\delta_{*i} \frac{P_{*i-1}^2}{P_{*i}} - \delta_{*i} P_{*i}\right)(a_i\cos\omega t \cos\varphi + b_i \sin\omega t \sin\varphi) \right] + \frac{\ell}{2}(-a_i\omega\sin\omega t \cos\varphi$$

$$+ b_i\omega\cos\omega t \sin\varphi - a_{i+1}\omega\sin\omega t \cos\varphi + b_{i+1}\omega\cos\omega t \sin\varphi) \tag{16}$$

For the n stage labyrinth seal, Eqs.(15) and (16) are represented in matrix form as;

$$\mathbb{T}\dot{u} + \mathbb{V}u' + \mathbb{A}u = \mathbb{G}_1\Big[a_* \cos(\varphi + \omega t) + a_* \cos(\varphi - \omega t) - b_* \cos(\varphi + \omega t)$$
$$+ b_* \cos(\varphi - \omega t)\Big] + \mathbb{G}_2\Big[-a_* \sin(\varphi + \omega t) + a_* \sin(\varphi - \omega t) + b_* \sin(\varphi + \omega t)$$
$$+ b_* \sin(\varphi - \omega t)\Big] + \mathbb{G}_3\Big[\theta_a \cos(\varphi + \omega t) + \theta_a \cos(\varphi - \omega t) - \theta_b \cos(\varphi + \omega t)$$
$$+ \theta_b \cos(\varphi - \omega t)\Big] + \mathbb{G}_4\Big[-\theta_a \sin(\varphi + \omega t) + \theta_a \sin(\varphi - \omega t) + \theta_b \sin(\varphi + \omega t)$$
$$+ \theta_b \sin(\varphi - \omega t)\Big] \tag{17}$$

where $P_{*0} = P_0$ (inlet pressure) and $P_{*n} = P_n$ (outlet pressure).

ANALYSIS

Analysis of Steady State

Setting the perturbation terms ξ_i and l_i zero in Eqs.(15) and (16) in order to obtain the pressure and peripheral velocity of each seal stage in steady state,

$$q_{i+1} = q_i = q_* \tag{18}$$

$$q_{i+1}\omega_i - q_i\omega_{i-1} + \tau'U_i' - \tau''U_i'' = 0 \tag{19}$$

As the multi labyrinth stage is considered as a serial nozzle, the axial flow rate in the steady state is obtained as follows

$$q_i = \alpha \delta_i \sqrt{\frac{2n}{n-1} P_{i-1}' \rho_{i-1}' \left[\left(\frac{P_i}{P_{i-1}}\right)^{\frac{2}{n}} - \left(\frac{P_i}{P_{i-1}'}\right)^{\frac{n+1}{n}}\right]} \tag{20}$$

where P_{i-1}' is the pressure of (i-1)th chamber which is taken into account of draughty flow. The pressure is given by Ref.(3) as;

$$P_i' = P_i + (P_0 - P_{*1})(1 - A_i^2)\xi_p l_p \quad , \quad l_p = \frac{2A_i}{A_i + 1} \tag{21}$$

where A_i is determined by the shape of labyrinth seal;

$$A_i = \frac{\frac{\delta_i}{l} C_c}{\frac{\delta_i}{l} C_c + \tan\theta} \tag{22}$$

where C_c is coefficient of vena contracta.
From these equations, state variables i.e. the pressure and flow rate satisfied the equilibrium condition, is obtained by iterating Eqs.(18) and (19). The peripheral velocity is obtained by using Eq.(19) in the same manner.

Referring to the left term in Eq.(17), the solutions are assumed as follows

$$P_i = P_{*i} + P_{*i}\left\{A_{+i}\sin(\varphi+\omega t)+B_{+i}\cos(\varphi+\omega t)+A_{-i}\sin(\varphi-\omega t)+B_{-i}\cos(\varphi-\omega t)\right\} \tag{23}$$

$$C_i = C_{*i} + C_{*i}\left\{E_{+i}\sin(\varphi+\omega t)+F_{+i}\cos(\varphi+\omega t)+E_{-i}\sin(\varphi-\omega t)+F_{-i}\cos(\varphi+\omega t)\right\} \tag{24}$$

Representing the above coefficients in matrix form as

$$\alpha_1 = \begin{bmatrix} A_{+1} \\ E_{+1} \\ \vdots \\ A_{+n} \\ E_{+n} \\ 0 \end{bmatrix} \quad, \quad \alpha_2 = \begin{bmatrix} A_{-1} \\ E_{-1} \\ \vdots \\ A_{-n} \\ E_{-n} \\ 0 \end{bmatrix} \quad, \quad \beta_1 = \begin{bmatrix} B_{+1} \\ F_{+1} \\ \vdots \\ B_{+n} \\ F_{+n} \\ 0 \end{bmatrix} \quad, \quad \beta_2 = \begin{bmatrix} B_{-1} \\ F_{-1} \\ \vdots \\ B_{-n} \\ F_{-n} \\ 0 \end{bmatrix}$$

the solution is written as;

$$u = \alpha_1 \sin(\varphi+\omega t)+\beta_1\cos(\varphi+\omega t)+\alpha_2\sin(\varphi-\omega t)+\beta_2\cos(\varphi-\omega t) \tag{25}$$

Substituting Eq.(25) into Eq.(17), and separating it to the elements $\cos(\varphi+\omega t)$, $\sin(\varphi+\omega t)$, $\cos(\varphi-\omega t)$ and $\sin(\varphi-\omega t)$, the coefficients are represented as follows;

$$\omega T\alpha_1 + V\alpha_1 + A\beta_1 = G_1 a_* + G_3\theta_a + G_5 b_* + G_7\theta_b \tag{26}$$

$$-\omega T\beta_1 - V\beta_1 + A\alpha_1 = G_1 a_* + G_4\theta_a + G_6 b_* + G_8\theta_b \tag{27}$$

$$-\omega T\alpha_2 + V\alpha_2 + A\beta_2 = H_1 a_* + H_3\theta_a + H_5 b_* + H_7\theta_b \tag{28}$$

$$\omega T\beta_2 - V\beta_2 + A\alpha_2 = H_2 a_* + H_4\theta_a + H_6 b_* + H_8\theta_b \tag{29}$$

where $G_1 \sim G_8$ and $H_1 \sim H_8$ are coefficient matrices which is composed of the matrices B, C, F and G. Solving Eqs.(26),(27) and Eqs.(28), (29) simultaneously, $\alpha_1, \beta_1, \alpha_2$ and β_2 are obtained. Then velocity and pressure in the gland is calculated by substituting the coefficients into Eq.(23), and the flow induced force for whole seal is obtained by integrating the pressure for each gland. Representing the x and y direction force by P_x and P_y,

$$P_x = -R_s\sum_{i=1}^{n}\int_0^{2\pi}P_{*i}\,\xi_i\,\ell\cos\varphi\,d\varphi$$
$$P_y = -R_s\sum_{i=1}^{n}\int_0^{2\pi}P_{*i}\,\xi_i\,\ell\sin\varphi\,d\varphi \tag{30}$$

The flow induced force F and phase angle from x axis are described as

$$F = \sqrt{P_x^2 + P_y^2} \qquad \phi = \tan^{-1}\frac{P_y}{P_x} \tag{31}$$

Spring coefficients and damping coefficients are obtained from Eqs.(30) and (31) in the following matrix form;

$$
\begin{bmatrix} K_{xx} K_{xy} & & 0 \\ K_{yx} K_{yy} & & \\ & K_{\theta xx} K_{\theta xy} \\ 0 & K_{\theta yx} K_{\theta yy} \end{bmatrix} \begin{Bmatrix} x \\ y \\ \theta_x \\ \theta_y \end{Bmatrix} + \begin{bmatrix} C_{xx} C_{xy} & & 0 \\ C_{yx} C_{yy} & & \\ & C_{\theta xx} C_{\theta xy} \\ 0 & C_{\theta yx} C_{\theta yy} \end{bmatrix} \begin{Bmatrix} \dot{x} \\ \dot{y} \\ \dot{\theta}_x \\ \dot{\theta}_y \end{Bmatrix}
\tag{32}
$$

When Eqs.(30) and (31) are rewritten to Eq.(32) in the above, the following form is used as ξ_i,

$$
\xi_i = \xi_{1i}\, a_* \cos\omega t + \xi_{2i}\, a_* \sin\omega t + \xi_{3i}\, b_* \cos\omega t + \xi_{4i}\, b_* \sin\omega t + \xi_{5i}\, \theta_a \cos\omega t
$$
$$
+ \xi_{6i}\, \theta_a \sin\omega t + \xi_{7i}\, \theta_b \cos\omega t + \xi_{8i}\, \theta_b \sin\omega t
$$

Using the above expression, the following relations are obtained between coefficients;

$$
\begin{aligned}
&K_{xx}= K_{yy} \quad K_{\theta xx}= K_{\theta yy} \quad K_{xy}=-K_{yx} \quad K_{\theta xy}=K_{\theta yx} \\
&C_{xx}= C_{yy} \quad C_{\theta xx}= C_{\theta yy} \quad C_{xy}=-C_{yx} \quad C_{\theta xy}=-C_{\theta yx}
\end{aligned}
\tag{33}
$$

NUMERICAL EXAMPLE AND DISCUSSIONS

The labyrinth seal having three teeth, which is shown in Fig.2, is used as a numerical model. Details of the labyrinth seal is shown in Table 1 and for the parameter survey each element of seal dimension is independently changed in order to investigate the influence of its seal size on the flow induced force. In order to evaluate the seal force, circular orbit (a_* = b_* in Eq.(17)) are used as a whirling of labyrinth seal, and its radius a_* =0.1mm. For the calculation the following equation is used as the friction coefficient between rotor and stator;
for stator surface;

$$
Re_i' = \frac{D(U - C_{*i})}{\nu}
$$

where D is wetted perimeter length considered the rotating Reynold's Number

$$
Re_i' < 1200 , \quad \lambda_i' = 64/Re_i' , \quad Re_i' \geqq 1200 , \quad \lambda_i' = 0.3164\, Re^{-0.25}
$$

for rotor surface;

$$
Re_i'' = \frac{D(U-C_{*i})}{\nu} , \quad Re_i'' < 1200 , \quad \lambda_i'' = 64/Re_i' , \quad Re_i'' \geqq 1200 , \quad \lambda_i'' = 0.3164\, Re^{-0.25}
$$

Two methods are used for the numerical calculation, one is the method which is shown in previous section, the other is one which is the finite diference method that was proposed in Ref.(1). At first calculated results for these two methods are compared with and as the result it is known that these two results agree. Then parameter surveys of labyrinth seal are carried out to see the influence on the flow induced force which exits the instability.

In this paper critical speed of a rotor system is assumed to be 5000 rpm, and rotating speed of the rotor is represented in nondimensional expression as ω/ω_n(ω (rpm):rotating speed of the rotor). F and FAI shown in figures mean the absolute value of the force induced by labyrinth seal and its phase angle from x axis.

212

a) Accuracy of Two Calculation Method

Fig.3 shows the spring coefficients and damping coefficients which are obtained by two methods i.e. approximate method and finite difference method. In the figure, full line and broken line show the coefficients for inlet pressure P_0 =196.13(KPa) and 147.1(KPa) respectively and outlet pressure Pn=98.07(Kpa) which are obtained by the approximate method and doted line shows the coefficient for inlet pressure P_0=196.13(KPa) and outlet pressure P_3=98.0(KPa) which is obtained by the finite difference method. Also sign (-) on line means negative value. From this figure full line and dotted line coincide very well so each calculation method has good accuracy.

b) Influence of Deflection of Steady

In this paper pressure, peripheral velocity and flow rate in steady state are iteratively calculated, however, Kostyuk and other authors obtain them by another method and there are some discrepancies between both steady state values. Moreover, steady state values in field and the calculated values may have discrepancies. So it is important to investigate the influence of deflection from steady state on the accuracy of the induced force. Then Fig.4 shows the flow induced force and its phase angle when pressure is a little deflected from steady state where the number on lines correspond to the number in Table 3. The calculated data are shown in table 2. From the calculated result, it is known that even if the flow rate is deflected 20% from the steady state, flow induced force and phase angle are not so influenced, and these curves become like one line, so this figure is neglected. On the other hand if the pressure is deflected 0.5% from steady state value, they are influenced very much. Also it is known that the induced force is not influenced by rotating speed of rotor but if it is separated to component, influence of rotating speed is remarkable as shown in Fig.5. From the above discussions it is concluded that in the calculation of flow induced force, steady state values must be calculated with high accuracy.

c) Influence of Pressure Difference Between Inlet and Outlet

Fig.6 shows the influence of pressure difference between inlet and outlet on the flow induced force when inlet (entrance) pressure is kept constant value (209 atm) and outlet (exit) pressure is changed. The figure shows that as the outlet pressure becomes large, i.e. the pressure difference between inlet and outlet becomes small, the flow induced force becomes small. As the flow rate decreases, the induced force proportionally decreases.

d) Influence of Labyrinth Seal Radius

Fig.7 shows the influence of labyrinth seal radius on the flow induced force, where the seal radius is valiable and other dimensions are fixed at constant values. Here flow rate means total flow rate as shown in the expression;

From the figure the flow induced force proportionaly increases as the seal radius increases. Therefore, the flow induced force due to labyrinth seal can be easily evaluated by the similarity law, when the seal radius is known.

e) Influence of Seal Clearance

Fig.8 shows the relation between seal clearance and the flow induced force and the leakage flow rate (leakage mass flow rate per unit length), where as the clearance increases, the induced force F decreases and the flow rate increases proportionally.

213

f) Influence of Seal Pitch

Fig.9 shows the influence of seal pitch on the flow induced force, when strip height is kept constant. From the figure it is known that as the seal pitch increases, the induced force increases, but the leakage flow rate q does not so much changed. Thus the large pitch is not good from the view point of the flow induced force.

g) Influence of Number of Seal Chamber

Fig.10 shows the influence of chamber number on the induced force and the leakage flow rate, where inlet and outlet pressure is constant and each chamber dimension is also same. From the figure the induced force increases like hyperbolic as the chamber number increasing. On the other hand leakage flow rate decreased like exponentially. Therefore optimum number of chambers may be determined when inlet and outlet pressure are known.

h) Influence of Seal Strip Height

Fig.11(a)(b) shows the influence of seal strip height. In this case the induced force, phase angle and leakage flow rate do not influenced so much. But if this result is represented in the spring and damping coefficients, the influence due to the strip height is remarkable. Fig 11(c) shows the spring coefficients k_{xx} and k_{xy}.

i) Influence of Divergence and Convergence Type Labyrinth Seal

Fig.12 shows a comparison of seal types, that is, comparison of straight through type, convergence type and divergence type. In this calculation there is little discrepancies of the flow rate q, so its figure is neglected. From Fig.12(a), it is known that the flow induced force for the convergence type is the smallest of all and divergence type is the largest inspite of the same leakage flow rate. From Fig.12(c), the flow induced coupling stiffness k_{xx} is similar characteristics, but convergence type is excellent from the viewpoint of stability.

CONCLUSION

In this report the flow induced force due to labyrinth seal which is sometimes the cause of instability is studied for the special model. That is, the labyrinth seal of shroud of steam turbine is used as an example and its flow induced force and stiffness and damping coefficients are theoretically calculated by two method. Then influences of deflection of steady state, pressure difference between inlet and outlet, labyrinth seal radius, seal clearance, seal pitch, number of seal chamber and seal strip height on the flow induced force and leakage flow rate are investigated. As the results, it is known that the above factors are very influential on the flow induced force. However further theoretical and experimental investigation are required in order to obtain a more precise description of labyrinth seal characteristics.

REFERENCES

1. Iwatsubo, T. : Evaluation of Instability Forces of Labyrinth Seals in Turbines or Compressors. NASA 2133, May 12-14, 1980.

TABLE 1. - LABYRINTH SEAL DIMENSIONS FOR NUMERICAL EXAMPLE

SEAL RADIUS	R_s	1	(m)
ROTOR NATURAL FREQUENCY	ω_n	5000	(rpm)
STRIP HEIGHT	h	10	(mm)
SEAL CLEARANCE	δ	1.3	(mm)
STRIP PITCH	ℓ	30	(mm)
NUMBER OF CHAMBER	N	2	
SEAL TYPE		straight-through type	

TABLE 2. - GAS CONDITION FOR NUMERICAL EXAMPLE

OPERATING LIQUID		air	
LIQUID TEMPERATURE	T	784.15	(K)
ENTRANCE PRESSURE	P_o	20482.0	(kPa)
EXIT PRESSURE	P_n	19678.4	(kPa)

TABLE 3. - DEFLECTION OF PRESSURE AND FLOW RATE FROM STEADY STATE

		PRESSURE OF EACH STAGE (kPa)				FLOW RATE
		PO	P1	P2	P3	(kg s/m^2)
STEADY STATE VALUE	(1)	20482.0	20166.3	19936.7	19678.4	6.8443
DEFLECTION OF	(2)	20482.0	20267.2	20036.4	19678.4	6.8443
PRESSURE P1,P2	(3)	20482.0	20065.5	19836.9	19678.4	6.8443
DEFLECTION OF	(2)	20482.0	20166.3	19936.7	19678.4	7.5287
FLOW RATE	(3)	20482.0	20166.3	19936.7	19678.4	6.1599

215
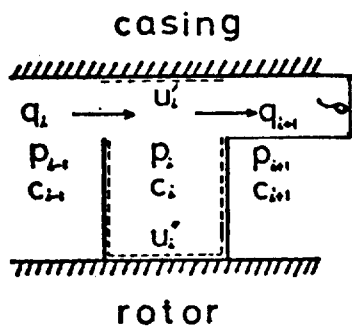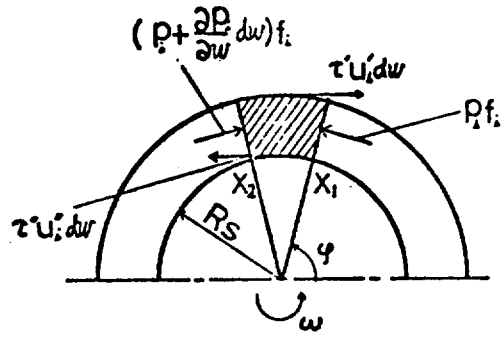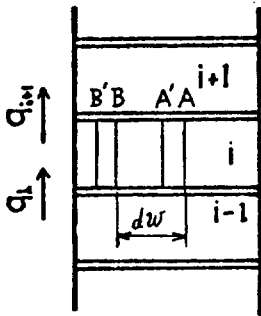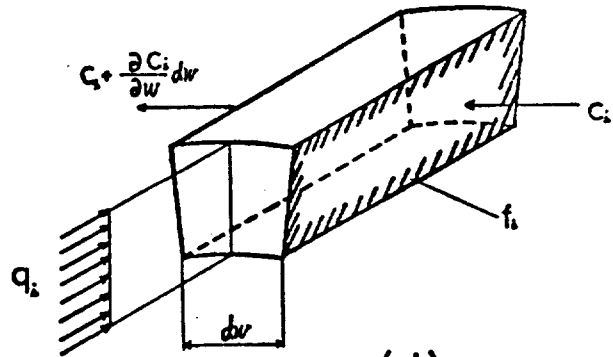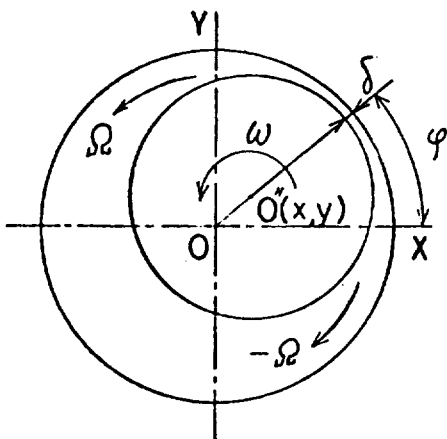
Figure 1. - Cross section of labyrinth seal
and definition of the coordinate.
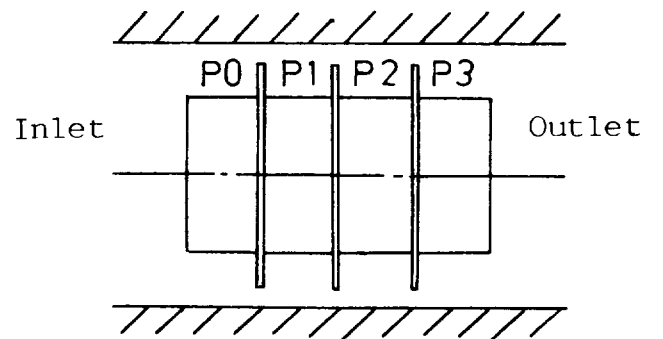
Figure 2. - Labyrinth seal model
for numerical example.
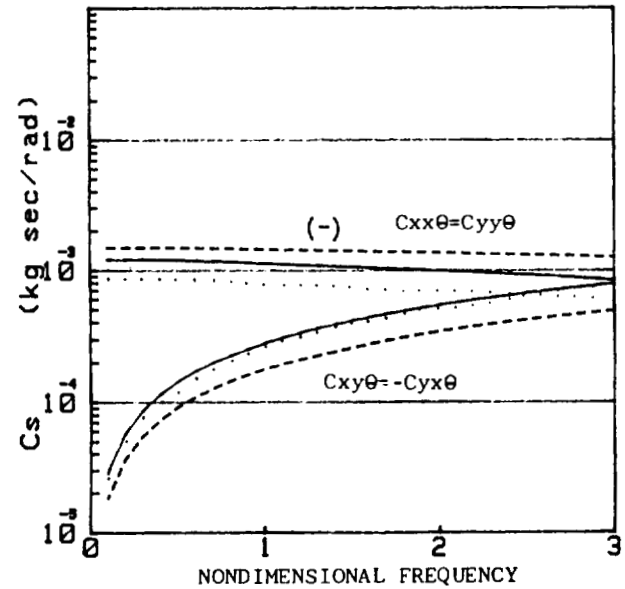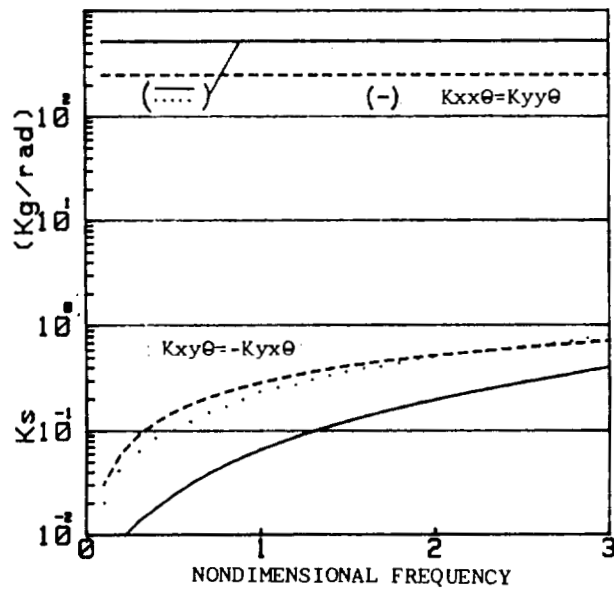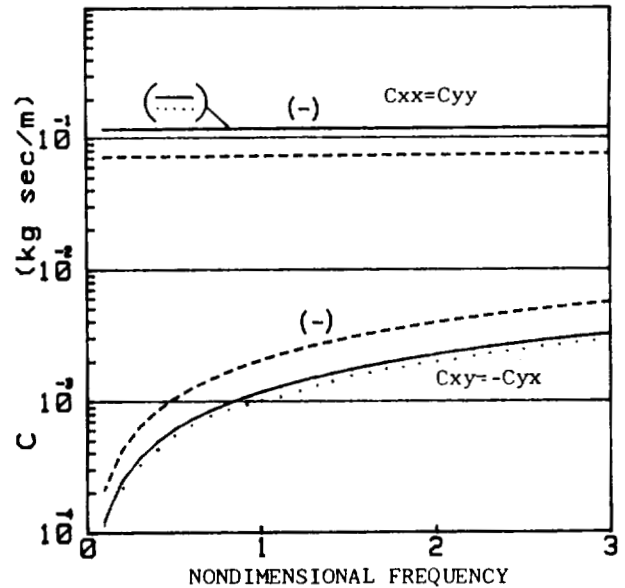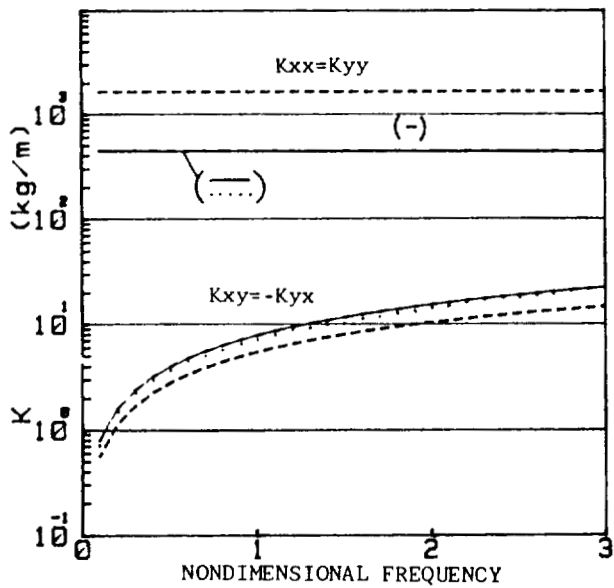
Figure 3. - Accuracy of two calculating methods and influence of pressure difference between inlet and outlet.
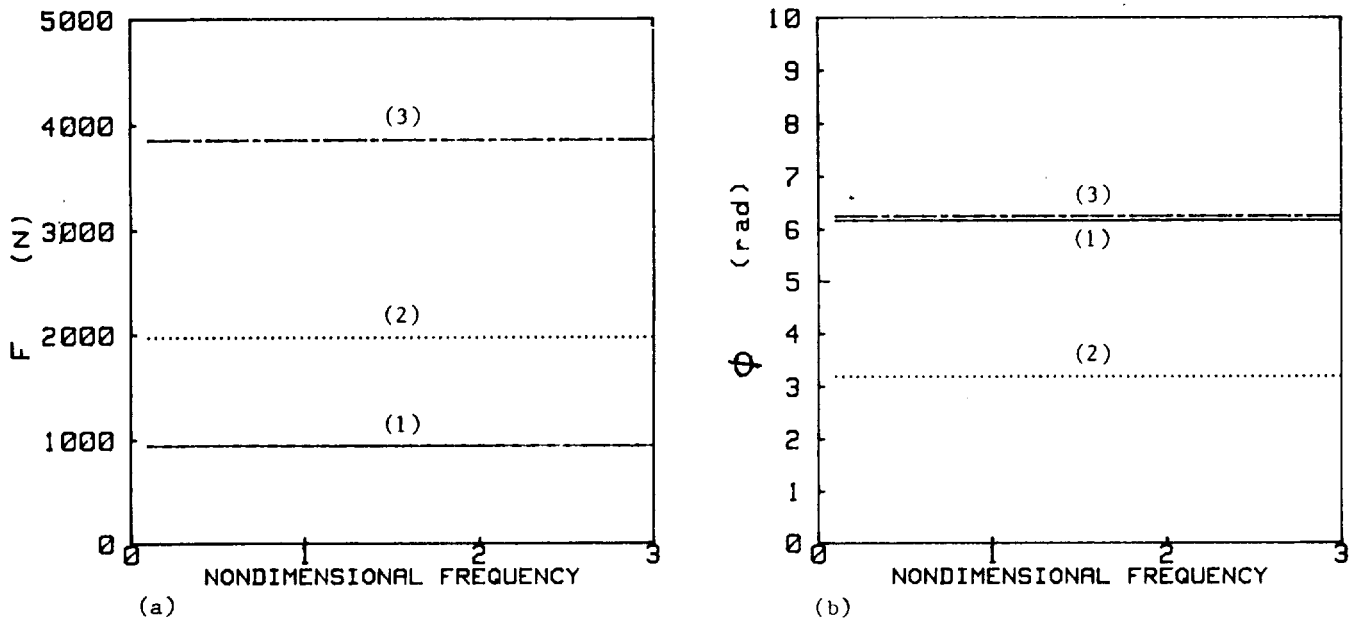
Figure 4. - Influence of pressure deflection from steady state on
the flow induced force.
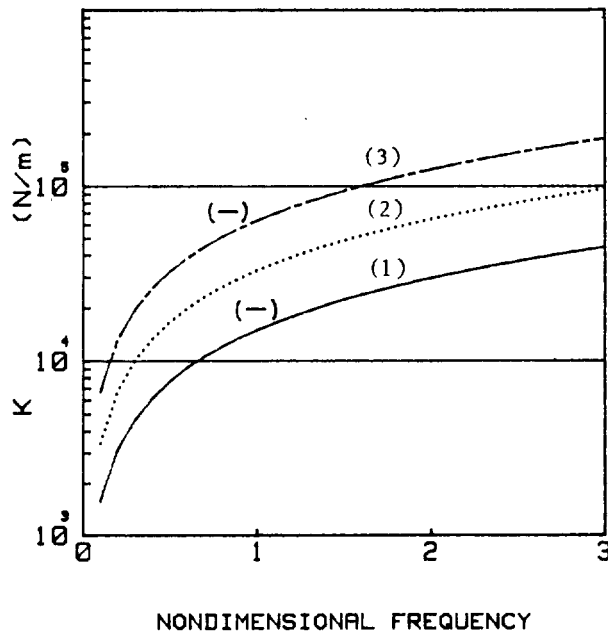
Figure 5. - Influence of pressure deflection from steady state on
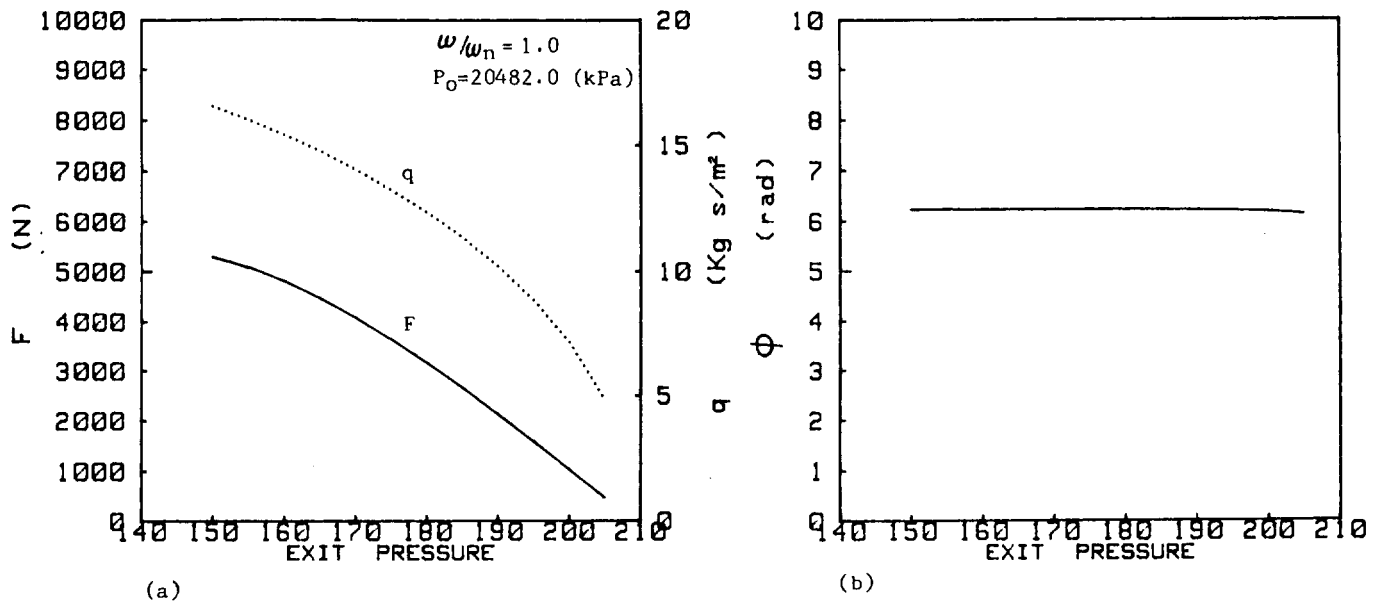the cross coupling stiffness.
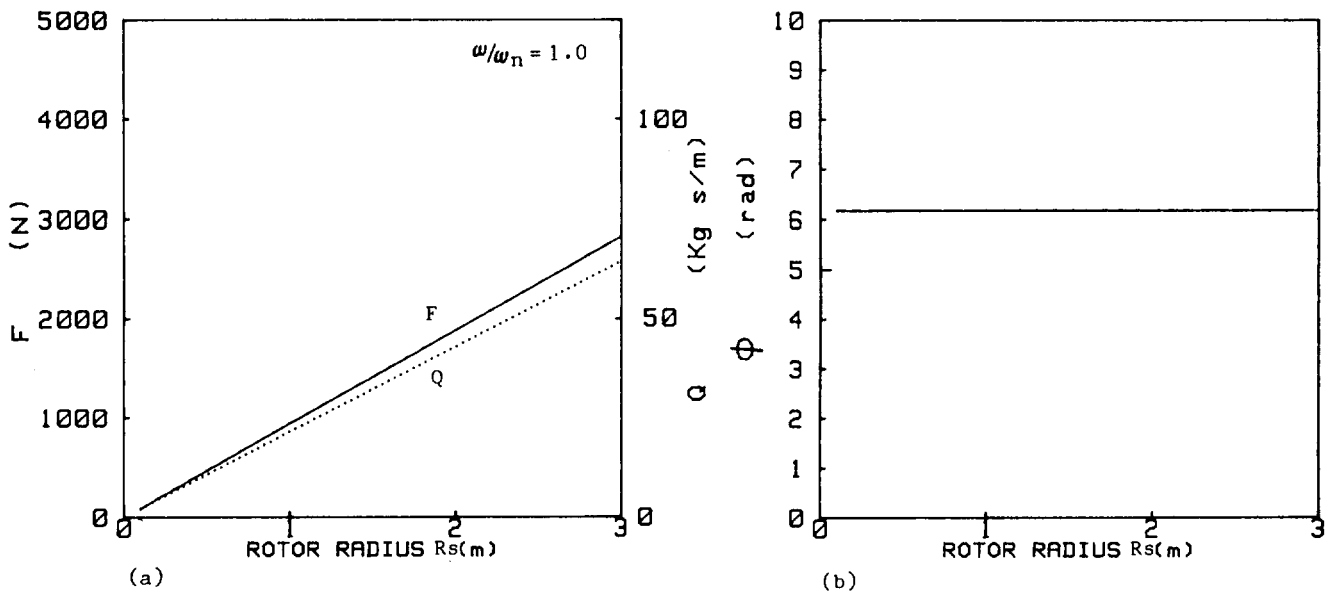
Figure 6. - Influence of pressure difference between inlet and outlet.

Figure 7. - Influence of labyrinth seal radius.
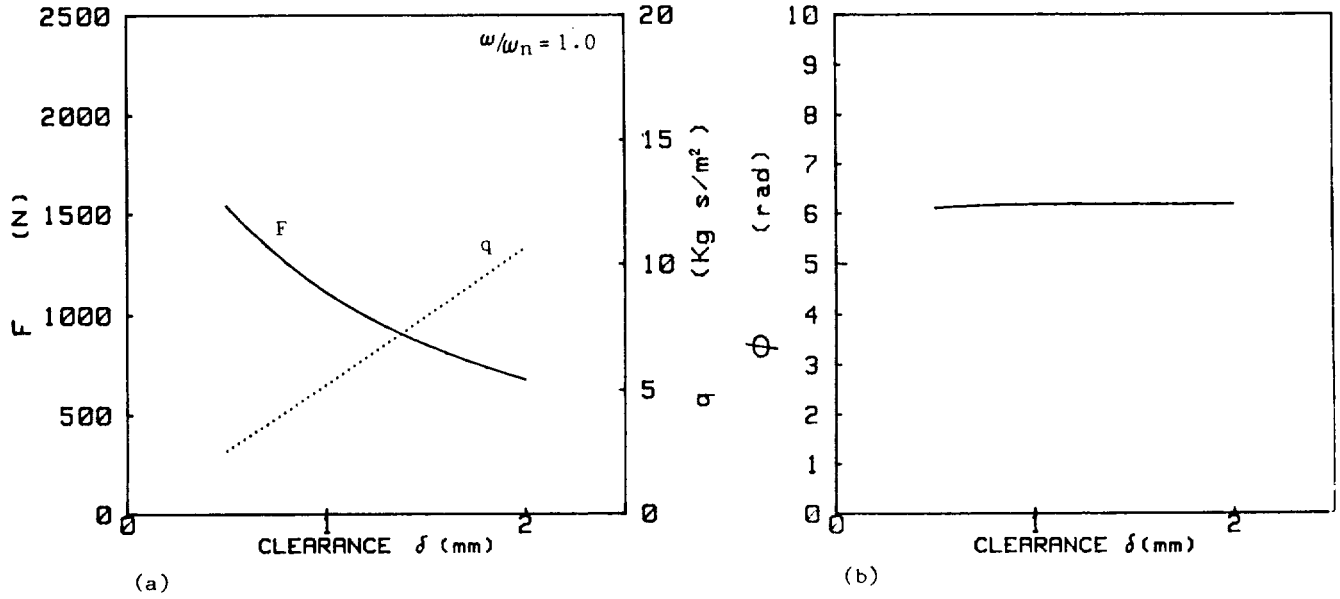
Figure 8. - Influence of seal clearance.
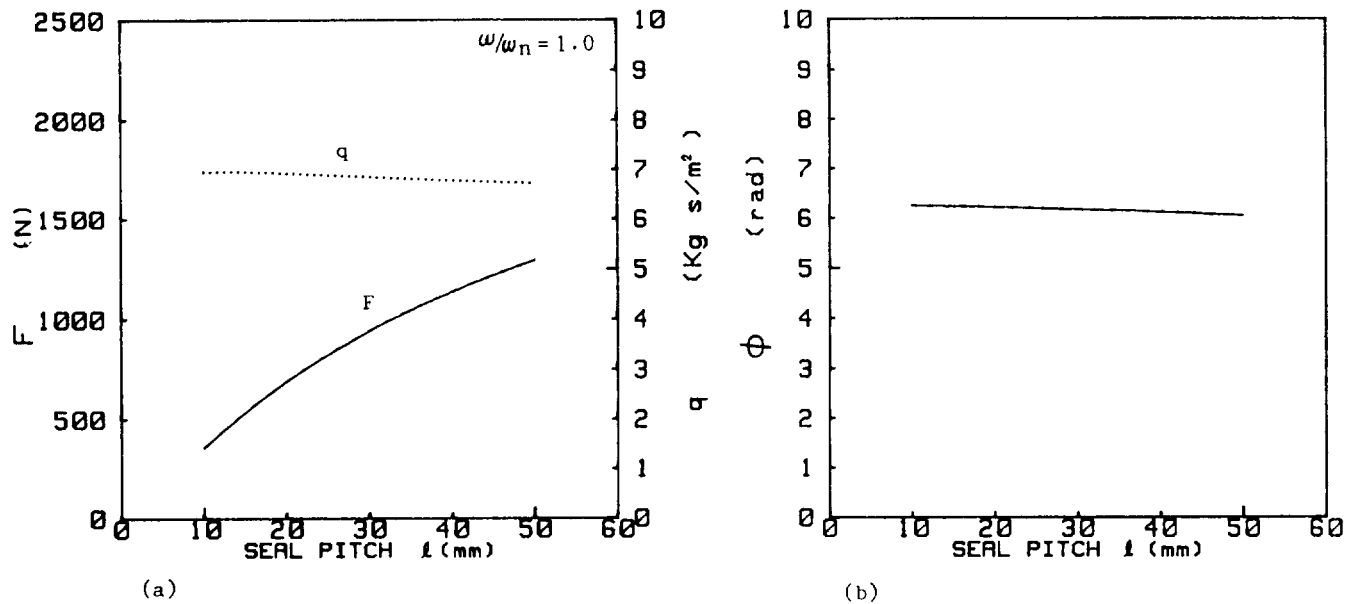
Figure 9. - Influence of seal pitch length.
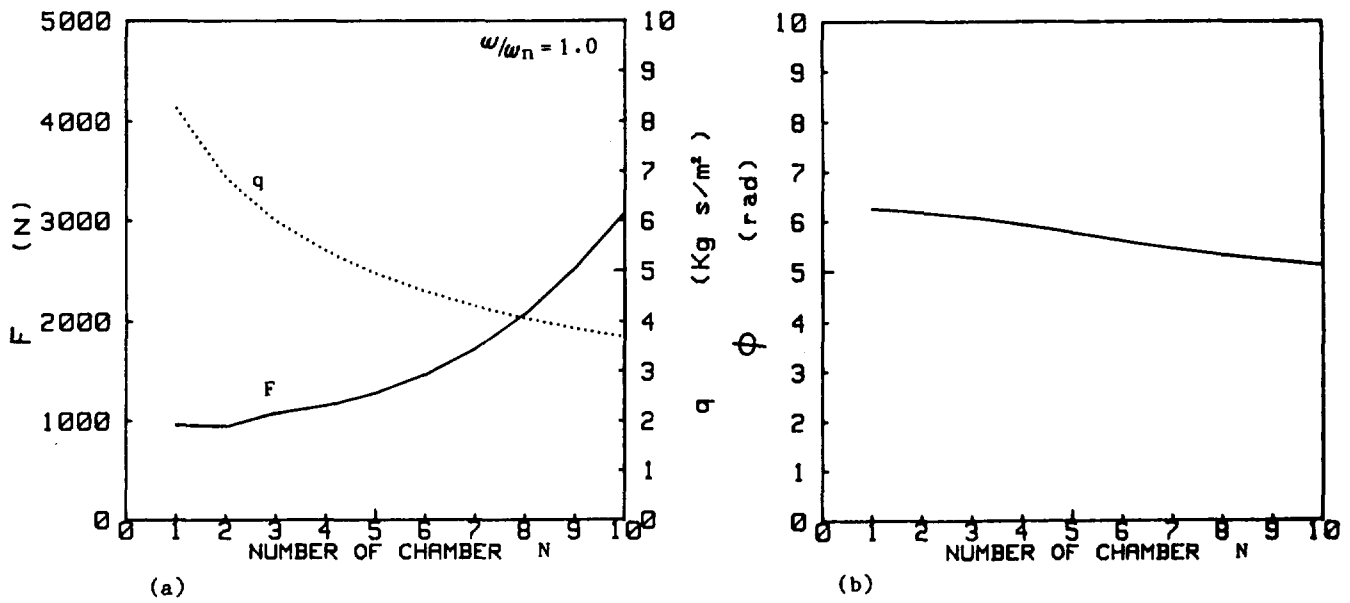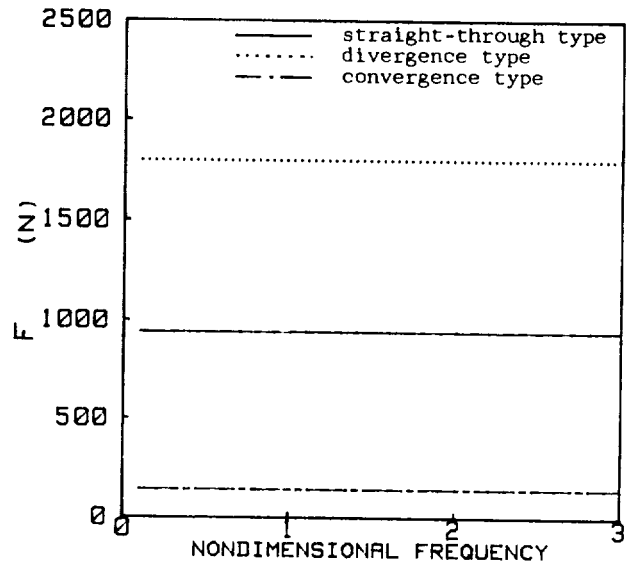
Figure 10. - Influence of number of seal chamber.
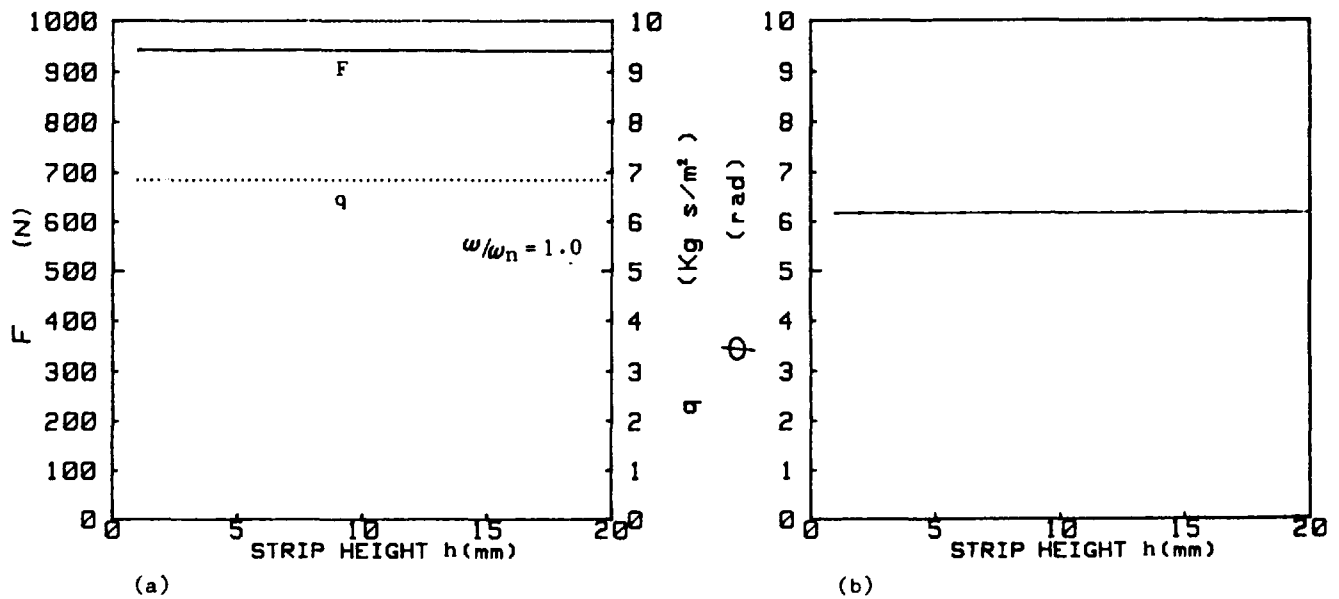
Figure 11. - Influence of seal strip height on the flow induced
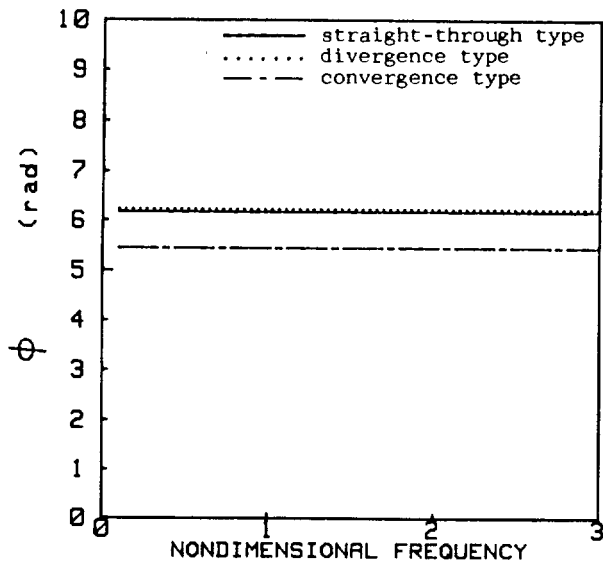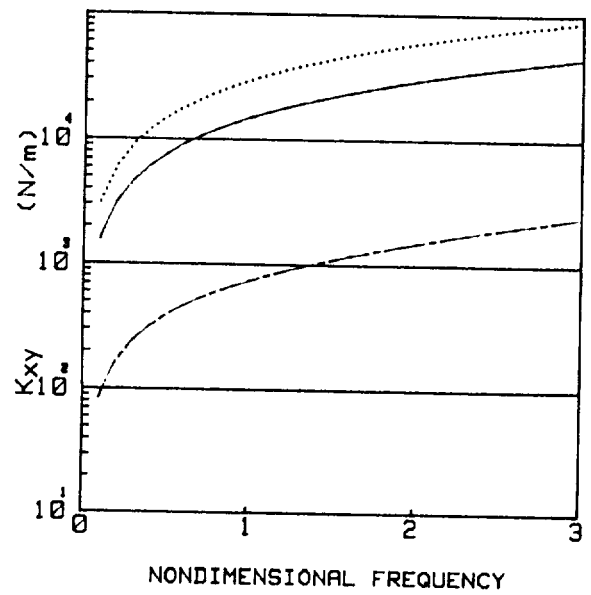force and phase angle.

221
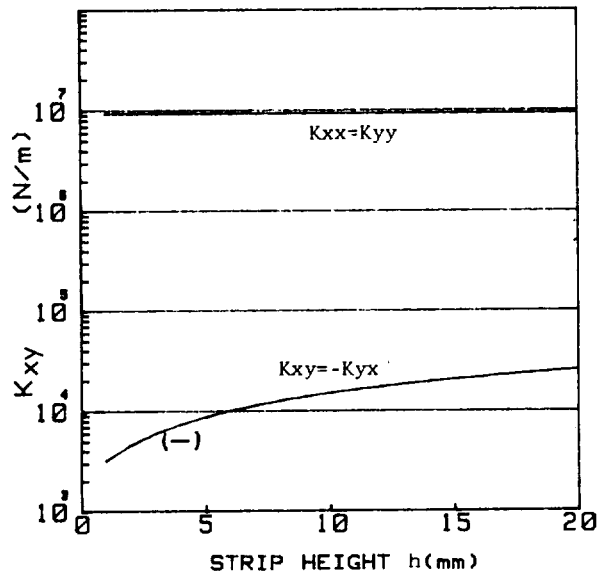
Figure 11. - Influence of seal strip
height on flow induced cross-coupling.

(a)

(b)

(c)

Figure 12. - Influence of divergence and convergence type labyrinth seal.